BUTTERWORTH HEINEMANN

Polymer Vol. 36 No. 15, pp. 2895–2902, 1995

0032-3861/95/$10.00+0.00

Applications of a dilatational yielding model to rubber-toughened polymers

A. Lazzeri
Centre for Materials Engineering, University of Pisa, Pisa 56100, Italy

and C. B. Bucknall*
Advanced Materials Group, Cranfield University, Bedford, MK43 0AL, UK
(Received 6 January 1994; revised 18 April 1994)

A model for dilatational yielding in rubber-toughened polymers, which was proposed in an earlier paper, is developed further. According to the model, deformation begins with cavitation of the rubber particles, and progresses through the growth of dilatational bands, which are cavitated planar yield zones combining in-plane shear with extension normal to the band. The model is used to predict band angles and other characteristics of yielding in toughened plastics, including the conditions under which polymers yield without cavitating. Electron micrograph evidence for the formation of dilatation bands is presented, and the influence of these bands on deformation and fracture behaviour is discussed, using a novel method of presentation based on cavitation diagrams.

(Keywords: rubber toughening; yielding; dilatation)

INTRODUCTION

In a previous paper[1], we proposed a new quantitative model for dilatational yielding in rubber-toughened plastics, based on cavitation of the rubber particles followed by the formation of *dilatation bands*. This term describes planar yield zones that combine in-plane shear with cavitational extension in the direction normal to the plane. Dilatation bands have been observed many times in metals, especially at crack tips, and the relevant theory, based originally on work by McClintock[2], has been developed by Berg[3], Gurson[4], Tvergaard[5], Dung[6] and others. A recent book by Thomason reviews the subject in some detail[7].

Cavitation in metals generally originates at defects or hard inclusions. Subsequent void growth occurs as a result of plastic deformation in adjacent regions of the metallic matrix. By contrast, cavitation in toughened plastics originates within the rubber particles. According to the new dilatation model, the mechanism responsible for particle cavitation is essentially elastic, and results in each particle losing some or all of its initial resistance to further dilatation. As the volume fraction of particles may be 20% or more, this means that the *effective* void content may under certain conditions jump suddenly from zero to 20% at comparatively small strains. The abruptness of the change depends upon particle size distribution. The degree to which cavitated particles behave like voids depends upon the properties of the rubber and the morphology of the particles.

The present paper reviews the model, and applies it to rubber-toughened plastics under various loading conditions, including stress fields at crack tips, in order to show how the formation of dilatation bands affects yield behaviour.

* To whom correspondence should be addressed

THE DILATATIONAL YIELDING MODEL

Cavitation of rubber particles

The new model is based upon a thermodynamic criterion for cavitation in rubber-toughened plastics, which specifies that particles cavitate when the available energy exceeds a critical value. For a rubber particle of radius R, subjected to an initial volume strain Δ_{v0}, the stored volumetric strain energy U_0 within the rubber phase is given by:

$$U_0 = \tfrac{4}{3}\pi R^3\left(\frac{\sigma_m \Delta_{v0}}{2}\right) = \tfrac{2}{3}\pi R^3 K_r \Delta_{v0}^2 \qquad (1)$$

where σ_m is the mean stress (sometimes called negative pressure or hydrostatic tension) in the rubber, and K_r is the bulk modulus of the rubber.

If the radius R is held constant, the formation of a cavity of radius r reduces the volume strain in the rubber phase to $(\Delta_{v0} - r^3/R^3)$, so that volumetric strain energy is released. On the other hand, it introduces two additional contributions to the energy of the rubber particle: the surface energy $4\pi r^2\Gamma$, where Γ is the specific surface energy of the rubber; and the shear strain energy required to stretch the rubber and allow the cavity to expand. The energy of the cavitated particle is then given by:

$$U = \tfrac{2}{3}\pi K_r R^3\left(\Delta_{v0} - \frac{r^3}{R^3}\right)^2 + 4\pi r^2\Gamma + 2\pi r^3 G_r F(\lambda_f)$$

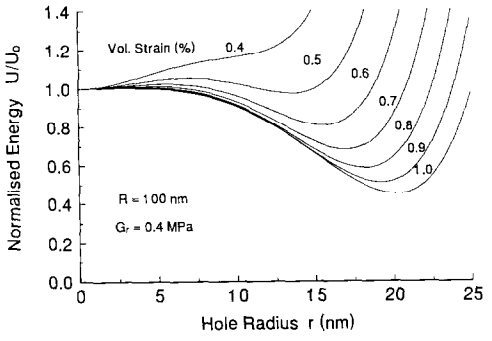

Figure 1 Relationship between energy of rubber particle and void size, calculated from equation (2) for a range of initial volume strains. Rubber properties as given in the text

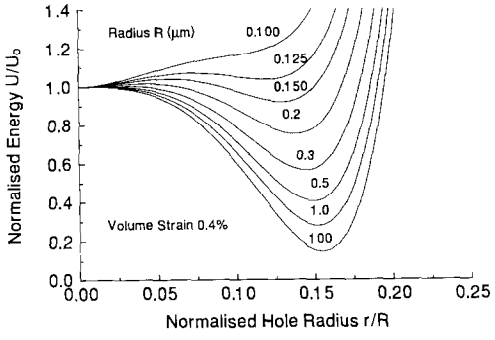

Figure 2 Relationship between energy of rubber particle and void size, calculated from equation (2) for a range of particle sizes. Rubber properties as in *Figure 1*

$$\frac{U}{V_r} = \frac{3U}{4\pi R^3} = \frac{K_r}{2}\left[\Delta_{v0} - \left(\frac{r}{R}\right)^3\right]^2 + \frac{3\Gamma}{R}\left(\frac{r}{R}\right)^2 + \frac{3G_r F(\lambda_f)}{2}\left(\frac{r}{R}\right)^3 \quad (2)$$

The rubber stretching term is proportional to the shear modulus of the rubber, G_r, and to $F(\lambda_f)$, where λ_f is the extension ratio at failure for the rubber under biaxial stretching conditions. The function $F(\lambda_f)$ is derived in the earlier paper[1].

The conditions necessary for the expansion of small cracks, bubbles and other defects in rubbers have been studied and analysed extensively by Gent and coworkers[8–12] and by Williams and Schapery[13]. Using a fracture mechanics approach, they show that the critical dilatant stress increases as the volume of loaded material decreases, and becomes dependent upon surface energy and upon large-strain properties of the rubber as the defect size decreases. The rubber particle cavitation model applies the same approach, but extends the principle to rubber particles that contain no defects larger than the typical intermolecular spacing.

The relationship between U/U_0 and r/R described by equation (2) is illustrated in *Figures 1* and *2*, with $G_r = 0.4\,\text{MPa}$, $K_r = 2\,\text{GPa}$, $\Gamma = 0.03\,\text{J m}^{-2}$ and $F(\lambda_f) = 1$. For these typical values of G_r and K_r, Poisson's ratio ν is 0.499 90. Cavitation occurs at a critical volume strain Δ_{v0}, which is inversely related to particle size[14], as can be seen from the rearranged version of equation (2), where the energy per unit volume of rubber, U/V_r, is expressed in terms of the dimensionless variable r/R. The absolute value of particle radius R affects only the surface energy term, which therefore becomes more important as particle size decreases. Thus the model predicts that, under an increasing stress applied to a rubber-toughened polymer, cavitation will begin in the largest particles, and progressively affect the smaller ones. The value of Γ chosen in the calculations represents the surface energy of a hydrocarbon liquid. For a crosslinked rubber, a somewhat higher energy would be appropriate, to take account of bond rupture. However, the surface energy necessary to form a small void is much smaller than the tearing energy of a typical macroscopic rubber sample, which dissipates energy viscoelastically over a region that often extends several millimetres from the crack tip.

Until it cavitates, each particle is strongly resistant to volumetric expansion because of its relatively high bulk modulus. However, this resistance is reduced on cavitation. Since in the present simplified treatment R is taken to be constant during this step, a particle of volume V_p may exhibit behaviour similar to that of a void of volume V_p, although the volume of the real void formed within the particle is only of the order of $0.01V_p$. A concentration of cavitated particles, having a *local* volume fraction f within a small planar zone, is the starting point for the propagation of a dilatational band. Such a band is similar to a dislocation, in that it generates an enhanced stress and strain field around its edge boundary. This can cause cavitation in particles that would otherwise be too small to respond in this way.

Yield criteria

The analysis of yielding in porous ductile materials proposed by Berg[3], and developed later by Gurson[4], is based on the von Mises equation, which gives the following expression for the *effective stress* σ_e at yield:

$$\sigma_e \equiv \left(\frac{(\sigma_1 - \sigma_2)^2 + (\sigma_2 - \sigma_3)^2 + (\sigma_3 - \sigma_1)^2}{2}\right)^{1/2} = \sigma_y \quad (3)$$

where σ_1, σ_2 and σ_3 are principal stresses, and σ_y is the yield stress in uniaxial tension (or compression) Equation (3) defines a cylinder in principal stress space with its axis at $\sigma_1 = \sigma_2 = \sigma_3$ (i.e. $\sigma_e = 0$), as illustrated in *Figure 3*. Equation (3) may also be expressed in terms o

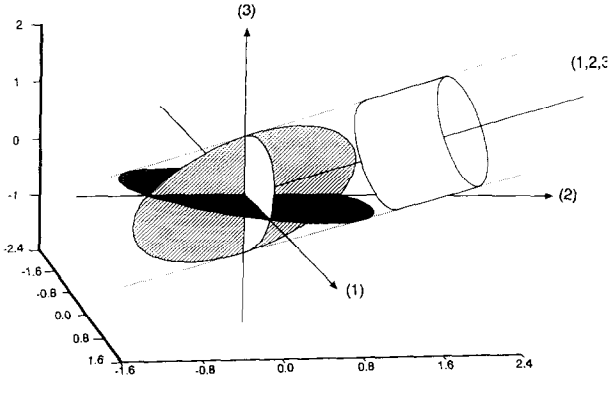

Figure 3 Representation in principal stress space of the von Mis yield criterion (equations (3) and (4)). Ellipses show projections on the 1–2, 1–3 and 2–3 planes

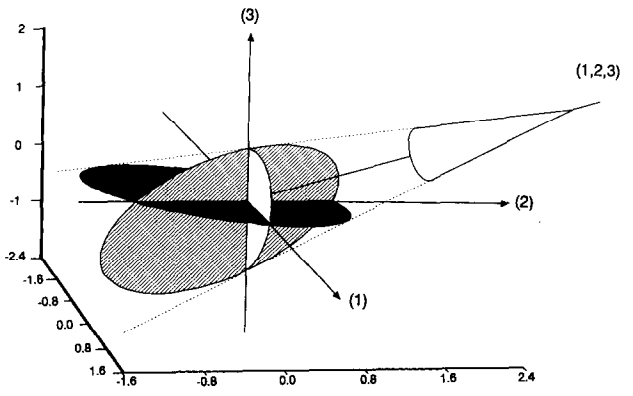

Figure 4 Representation in principal stress space of the pressure-modified von Mises yield criterion (equation (5)), with $\mu = 0.39$

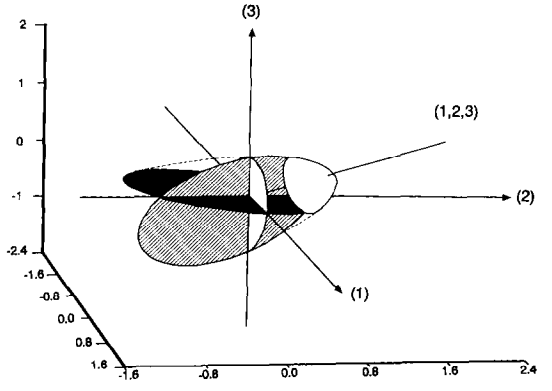

Figure 5 Representation in principal stress space of the pressure-modified von Mises yield criterion (equation (8)) for a cavitated polymer containing 20 vol% voids, with $\mu = 0.39$

the *plastic potential* Φ:

$$\Phi = (\sigma_e^2/\sigma_y^2) - 1 = 0 \qquad (4)$$

When the stress state is within the yield surface defined by equations (3) and (4) (Φ negative), the material behaves elastically. On reaching the yield surface at $\Phi = 0$, the material may flow at constant stress (elastic/perfectly plastic behaviour), or begin to strain-harden, in which case additional constitutive equations are needed.

Polymers deviate from classical von Mises behaviour, in that Φ is a function of the mean stress σ_m, where $\sigma_m = (\sigma_1 + \sigma_2 + \sigma_3)/3$. Various modifications of the von Mises equation have been proposed for ductile plastics, of which the following is best supported by experimental evidence[15]:

$$\sigma_e^2 = (\sigma_0 - \mu\sigma_m)^2 \qquad (5)$$

Here μ is a dimensionless constant, and σ_0 is the yield stress when $\sigma_m = 0$. The corresponding yield function is:

$$\Phi(\sigma_e, \sigma_m) = \frac{\sigma_e^2}{\sigma_0^2} + \frac{\mu\sigma_m}{\sigma_0}\left(2 - \frac{\mu\sigma_m}{\sigma_0}\right) - 1 = 0 \qquad (6)$$

As shown in *Figure 4*, the yield surface defined by equations (5) and (6) is a cone in principal stress space. This diagram emphasizes a major limitation of equation (5): at high positive values of σ_m (tip of cone), it predicts yielding when the effective stress σ_e is zero. Obviously, cavitation and fracture will intervene before that state of stress is reached.

Gurson applied a continuum treatment to a cavitated ductile material containing a volume fraction f of voids, and obtained the following yield function[4]:

$$\Phi = \frac{\sigma_e^2}{\sigma_y^2} + 2f\cosh\left(\frac{3\sigma_m}{2\sigma_y}\right) - f^2 - 1 = 0 \qquad (7)$$

His analysis leads to the conclusion that yielding occurs through the formation of dilatation bands, which allow the original voids to expand as plastic flow occurs in the intervening ligaments.

Lazzeri and Bucknall combined equations (5) and (7) to obtain the following yield function for cavitated polymers[1]:

$$\Phi = \frac{\sigma_e^2}{\sigma_0^2} + \frac{\mu\sigma_m}{\sigma_0}\left(2 - \frac{\mu\sigma_m}{\sigma_0}\right) + 2f\cosh\left(\frac{3\sigma_m}{2\sigma_0}\right) - f^2 - 1 = 0 \qquad (8)$$

This gives a round-nosed cone in stress space, as shown in *Figure 5*. As in *Figure 4*, it shows yielding when $\sigma_e = 0$, but at this point the material is no longer a continuum, and such yielding is physically possible. Locally within the ligaments surrounding the voids, the stress state is not purely triaxial, and plastic flow can occur.

Equation (8) contains two terms relating to dilatant yielding, one reflecting the flow behaviour within the continuous matrix polymer phase, and the other arising from the reduced constraints on yielding of the shear band when voids are present. Both terms are necessary, to ensure that equation (8) reduces to equation (6) when $f = 0$, and to equation (7) when $\mu = 0$. As the void content f increases, mean stresses within the ligaments remain tensile but become non-uniform, so that the term containing μ is then an approximation. However, the relative importance of this term diminishes with increasing void content, so that any error can be regarded as negligible.

Since the yield surfaces presented in *Figures 3–5* exhibit rotational symmetry, they can be represented more concisely in two dimensions, by choosing the symmetry axis as the abscissa, and drawing the generator of each surface. A modified version of such a representation, in which σ_e is plotted against σ_m for the three cases, is shown in *Figure 6*. This type of plot is helpful in discussing the effects of cavitation upon yielding in rubber-modified polymers. As the angle

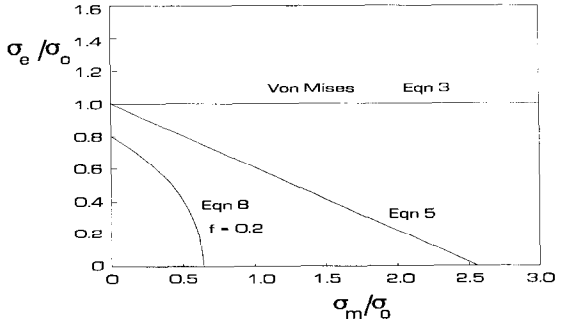

Figure 6 Foreshortened two-dimensional representations of yield surfaces shown in *Figures 3–5*

between the symmetry axis and each principal stress axis is $\cos^{-1}(1/\sqrt{3})$, each point on the curves shown in *Figure 6* must be shifted along the abscissa by a factor $\sqrt{3}$ in order to obtain the true generator for the corresponding yield surface.

APPLICATION OF MODEL TO TOUGHENED PLASTICS

Dilatation bands

An example of a dilatation band in a toughened thermoplastic is shown in *Figure 7a*. The section is taken from an injection-moulded Charpy specimen of rubber-toughened nylon-6, containing particles of polybutadiene. The bar was moulded and tested by Dijkstra and Gaymans at the University of Twente[16] before being sent to Cranfield. An area at the edge of the whitened zone, at some distance from the notch tip, was chosen for examination in the transmission electron microscope. Ultrathin sections were cut at −120°C from an OsO_4-stained block, using a diamond knife mounted on a Reichert-Jung Ultracut E ultramicrotome.

The micrograph shows obvious cavitation in a line of closely spaced particles, all of which are relatively large compared with the rest of the population. The accompanying sketch (*Figure 7b*) indicates the combination of normal and shear displacements that have taken place in forming the band, and defines the band angle ψ with respect to the principal stress axes. Both dilatational and shear components produce a concentration of elastic strain at the edge of the dilatation band. The dilatation

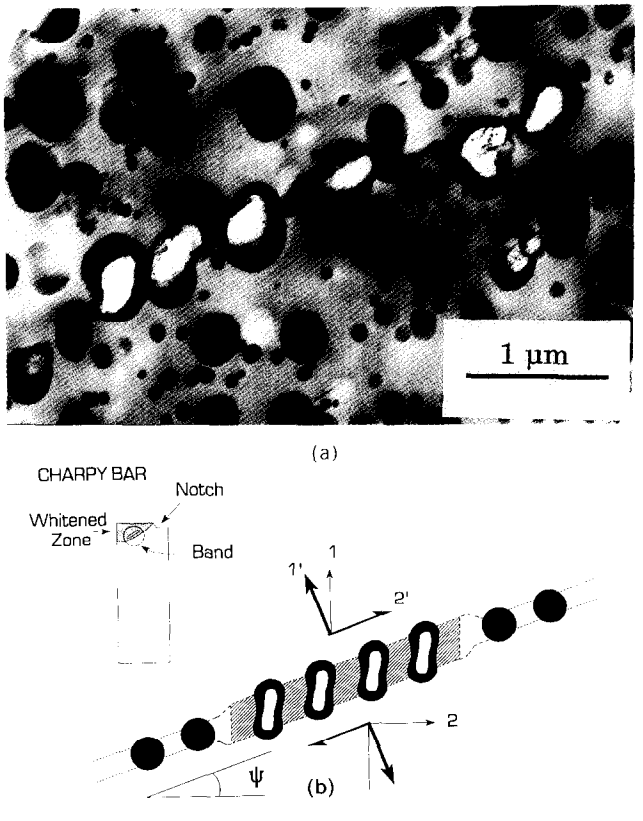

Figure 7 (a) Transmission electron micrograph of an OsO_4-stained ultrathin section from a fractured Charpy specimen of rubber-toughened nylon-6, showing a dilatation band. (Specimen courtesy of Gaymans and Dijkstra[10]. Microscopy: P. Logan.) (b) Sketch showing location of band in the broken Charpy bar and the strains within the band

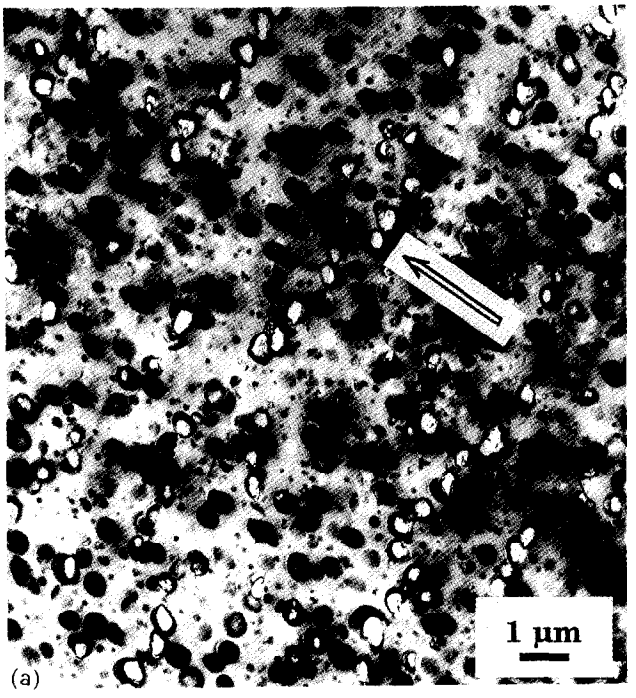

Figure 8 Lower magnification of specimen shown in *Figure 7*. Arrow indicates specimen axis (1 direction in *Figure 7*)

band will therefore propagate if the particles near its edge boundary are large enough, as discussed earlier. *Figure 8* is a micrograph taken at lower magnification, showing a set of parallel dilatation bands in the same ultrathin section.

The physical significance of these dilatation bands is that they alter the subsequent stress–strain behaviour of the material, especially at crack tips: cavitated rubber particles respond to dilatational stresses by increasing their volume substantially, whereas uncavitated particles do not. Dilatation bands thus enable the toughened plastic to yield and in some cases to strain-harden by internal cavitation, under conditions that would otherwise cause macroscopic necking or, where the material is under severe constraint at the tip of a sharp crack, allow only very limited plastic deformation. This point has been made by a number of previous authors, and is discussed in some detail by Huang and Kinloch[17].

Band angles

A Mohr's circle construction for determining the band angle ψ is shown in *Figure 9*. As indicated in *Figure 7b*, the normal to the band plane is defined as the 1′ direction and the in-plane shear direction as the 2′ direction. Plastic deformation rates can then be specified in terms of the strain rate $\dot{\epsilon}_{1'}$ normal to the band, and the two complementary shear strain rates $\dot{\epsilon}_{1'2'}$ and $\dot{\epsilon}_{2'1'}$. All other strain rates within the band, including $\dot{\epsilon}_{2'}$, are zero. Thus for a Mohr circle of strain rate in the 1–2 plane, the origin lies at $\dot{\epsilon}_{2'} = 0$, and the strain rates within the band are given by the intersection of the circle with the corresponding ordinate (points B_1 and B_2). The angle ψ between the band plane and the minor principal stress axis of the specimen (2 direction) is then obtained by drawing diagonals through B_1 and B_2.

From Berg's analysis[3]:

$$\cos(2\psi) = \frac{2\alpha\sigma_0}{\sigma_1 - \sigma_2} \tag{9}$$

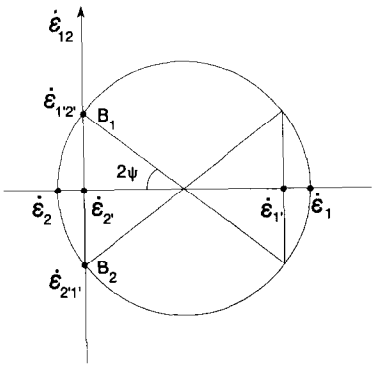

Figure 9 Mohr's circle of strain rate, showing method of calculating band angle ψ

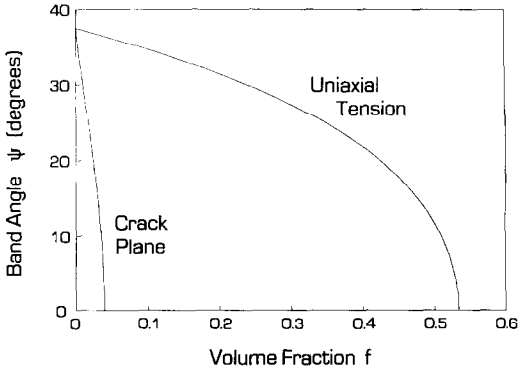

Figure 10 Relationship between band angle ψ and volume fraction of cavitated rubber particles in uniaxial tension and under full crack-tip constraint with $\sigma_1 = \sigma_2$, $\sigma_3 = 2\nu\sigma_1$. Calculations based on equation (8)

where, for a cavitated polymer exhibiting pressure-dependent yielding without strain hardening, α is given by[1,4]:

$$\alpha = \frac{\mu}{3}\left(1 - \mu\frac{\sigma_m}{\sigma_0}\right) + \frac{f}{2}\sinh\left(\frac{3\sigma_m}{2\sigma_0}\right) \qquad (10)$$

Figure 10 shows the relationship between band angle ψ and effective void content f, calculated using equations (9) and (10) for two cases of importance: uniaxial tension, and crack-tip plane-strain loading. In these calculations, the reference state $f = 0$ used in defining σ_0 is not the neat void-free matrix, but a material with 20 vol% of non-cavitated rubber particles. A typical value of 0.39 was used for the pressure coefficient μ, with Poisson's ratio $\nu = 0.4$. The figure shows that in the crack plane ψ tends to zero at effective current void contents f as low as 0.04. Consequently, the material is able to reach comparatively high strains in the process zone ahead of the crack tip, despite being subjected to severe constraints.

Consequences of particle cavitation

While it is obvious that voids and cavitated rubber particles reduce the yield stress of the parent polymer, following equation (8), it is not immediately clear whether their effects are greater than those obtained with the same volume fraction of non-cavitated rubber particles. In order to answer this question, it is necessary to have information about the yield behaviour of the non-cavitated rubber-toughened polymers as a function of particle volume fraction.

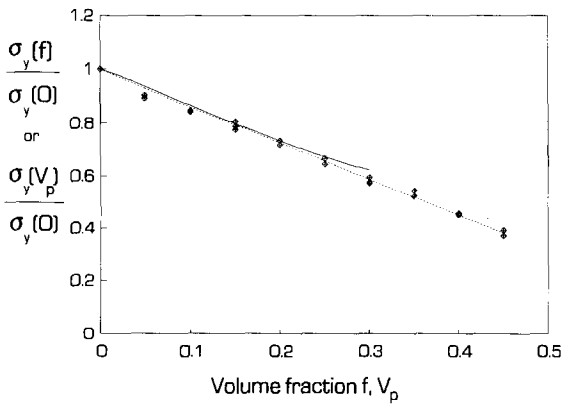

Figure 11 Comparison between Gurson's equation (full curve calculated from equation (7)) and data points of Gloaguen *et al.*[18] on yielding of rubber-toughened poly(methyl methacrylate) (PMMA) in uniaxial compression. The dotted straight line follows equation (11)

The most reliable experimental information about yielding of toughened plastics in the absence of cavitation comes from compression tests. Gloaguen *et al.*[18] have recently published comprehensive experimental data on σ_{yc}, the yield stress of rubber-toughened poly(methyl methacrylate) in uniaxial compression, for rubber particle volume fractions V_p in the range 0 to 0.45. To a good approximation, the relationship is linear, and fits the equation:

$$\sigma_{yc}(V_p) = (1 - 1.375V_p)\sigma_{yc}(0) \qquad (11)$$

A similar relationship can be taken to apply under other loading conditions, provided that there is no particle cavitation. In other words, σ_{yc} can be replaced with σ_0, so that equation (11) applies to non-cavitational yielding under all other stress states. Equation (11) and the compression yield data upon which it is based[18] are compared in *Figure 11* with the predictions of the modified Gurson equation (equation (8)) for the case of uniaxial tension. There is remarkably good agreement and, on the basis of this comparison, it would appear that fully dense rubber particles have almost exactly the same effect on tensile yield stress as that predicted for the equivalent volume of voids.

By contrast, non-cavitated particles are much less effective than voids in promoting yielding in the triaxial stress field at a crack tip. Here *cavitated* rubber particles behave like voids. This point is illustrated in *Figure 12*, which compares the relationship between yield stress and V_p given by equation (11) with those given by equation (8) for two specific stress states: uniaxial tension, and plane-strain crack-tip loading ($\sigma_1 = \sigma_2$; $\sigma_3 = 2\nu\sigma_1$) with Poisson's ratio $\nu = 0.4$.

Cavitation diagrams

Materials containing fully dense and cavitated rubber particles can conveniently be compared over a wide range of loading conditions by plotting effective stress at yield against mean stress, as illustrated in *Figure 13* for a material with a particle volume fraction $V_p = 0.2$. In pure shear ($\sigma_m = 0$), particle cavitation has no effect upon the yield stress, but as σ_m increases, the two curves diverge strongly.

In practice, as predicted by the cavitation model, holes form only when the rubber particles exceed a critical

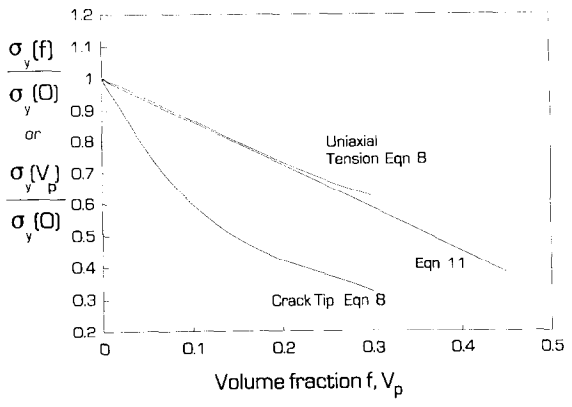

Figure 12 Relationship between yield stress and volume fraction of non-cavitated rubber particles (equation (11)), voids or cavitated rubber particles in a pressure-sensitive polymer under uniaxial tension (equation (8)) and voids or cavitated rubber particles in a pressure-sensitive polymer under full crack-tip constraint (also equation (8)). Note that the values of $\sigma_y(0)$ used to normalize the curves are different in each case

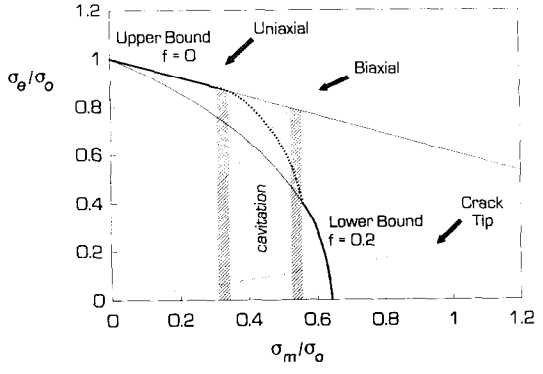

Figure 13 Schematic cavitation diagram showing transition (dotted curve) from yield envelope for 20 vol% non-cavitated rubber particles (upper straight line) to envelope for 20 vol% of fully cavitated rubber particles (lower curve). Shaded area indicates range of mean stresses required to cavitate rubber particles with a range of sizes

volume strain, which may or may not be reached before the material yields. Because the bulk modulus of a rubber is only about half that of a typical thermoplastic, Δ_v in the rubber particle is always a little higher than the volume strain in the polymer as a whole. A *cavitation diagram*, of the type illustrated schematically in *Figure 13*, is helpful in understanding how the yield surface is affected by void formation in the rubber particles. For each particle size, there is a critical volume strain, and therefore a critical mean stress σ_{mc}, at which cavitation occurs: the shaded region on the diagram indicates a range of σ_{mc} corresponding to a particular range of particle sizes. To the left of the shaded region, at low σ_m, there is no cavitation and the yield envelope follows the upper-bound curve (heavy line). To the right of the shaded region, where σ_m is relatively high, all of the particles cavitate before the material reaches its lower-bound yield stress, and the envelope conforms to the lower bound (heavy curve), which corresponds to the round-nosed cone shown in *Figure 5*. Within the shaded cavitation region, there is a transition from the upper- to the lower-bound curve (heavy dotted curve). Thus, if the particle size distribution is narrow enough, it is possible for a toughened polymer to be fully cavitated in the plane-strain zone of a crack tip ($\sigma_1 = \sigma_2 = \sigma$; $\sigma_3 = 0.8\sigma$; $\sigma_m = 2.8\sigma/3$), while being free from cavitation at the edge of the crack, where it is fully in plane stress ($\sigma_1 = \sigma_2 = \sigma$; $\sigma_3 = 0$; $\sigma_m = 2\sigma/3$).

When the particle sizes are reduced, or the shear modulus G_r of the rubber is increased, the shaded region shifts to the right, and the material may then yield (or fracture) under equi-biaxial stress before particle cavitation has occurred. The most important factor affecting the modulus is temperature: as the rubber is cooled through its T_g, G_r increases rapidly and the critical cavitation stress σ_{mc} rises sharply. At temperatures well above T_g, G_r varies more slowly, since it is proportional to T. On the other hand, as the temperature is raised, the yield stresses σ_e and σ_0 decrease relatively rapidly, while σ_{mc}, the critical mean stress for cavitation of the rubber particles, remains unchanged. The locations of the upper- and lower-bound curves in *Figure 13* are unaffected by temperature because both axes are normalized for σ_0, but the shaded cavitation region shifts to higher values as σ_0 decreases, with the result that, as the temperature is raised, it becomes easier to reach the yield point without cavitation. Finally, it should be noted that in some materials, such as nylon, the material may yield initially without cavitating, but subsequently begin to cavitate as the material strain-hardens and the true stress rises.

Relationship between volume strain and extension

Many laboratories have used dilatometric measurements to study deformation in rubber-toughened plastics under tensile loading. A standard method of data presentation is to plot volume strain Δ_v against extension ϵ_1 (ref. 19). In the absence of cavitation, and after subtracting the elastic contribution to strain, the resulting slope is usually zero. It may even be negative if the polymer undergoes strain crystallization. According to the mathematical theory of plasticity, materials that exhibit an increase in yield stress with increasing pressure will show a permanent increase in volume on undergoing plastic deformation. However, these effects are transient in polymers, and can be neglected in the present case[15].

The ratio in which an individual dilatation band contributes to the principal strains ϵ_1 and ϵ_2 in its plane of deformation may be obtained from the Mohr's circle of strain rate, as shown in *Figure 9*. The ratio of strain rates in the 1 and 2 directions is given by:

$$\frac{\dot{\epsilon}_2}{\dot{\epsilon}_1} = \frac{\cos(2\psi) - 1}{\cos(2\psi) + 1} = -\tan^2\psi \qquad (12)$$

Under uniaxial tension, ϵ_2 represents a decrease in the cross-sectional area A. the term $-\tan^2\psi$ is therefore equal to $\partial\Delta A/\partial\epsilon_1$. In an isotropic material, normals to shear and dilatation bands are distributed uniformly on a cone having its axis in the 1 direction. Both ϵ_2 and ϵ_3 then contribute equally to ϵ_1 and A, and the slope of the volume–extension curve can be obtained from:

$$\frac{d\Delta_v}{d\epsilon_1} = \frac{d\epsilon_1 + d\epsilon_2 + d\epsilon_3}{d\epsilon_1} = 1 + \frac{d\Delta A}{d\epsilon_1} = 1 - \tan^2\psi \qquad (13)$$

In the absence of cavitation, tensile specimens show a decrease in cross-sectional area with increasing strain, which often involves necking. The formation of dilatation bands alters this pattern of behaviour, by reducing the change in external cross-sectional area caused by a given extension. In the limit, when $\psi = 0°$, deformation may occur at constant cross-section.

DISCUSSION AND CONCLUSIONS

This paper provides evidence for the formation of dilatation bands in a rubber-toughened nylon containing polybutadiene particles, and information about their morphology. Electron microscopy shows that large rubber particles cavitate within approximately planar bands, undergoing shear in combination with extension normal to the band plane. These observations are consistent with the model proposed in our earlier paper[1].

The present study also examines the predictions of the cavitation and dilatation band models for rubber-toughened plastics. The theory shows that, immediately ahead of a sharp crack, materials containing quite low concentrations of cavitating particles ($f \leq 0.04$) can form bands parallel to the crack plane. Under different loading conditions, a toughened polymer may cavitate before yielding, or after yielding, or not at all, depending upon the relative positions of the yield envelope and the mean stress range over which particle cavitation occurs. These relationships can conveniently be represented in a cavitation diagram, which has effective stress as ordinate and mean stress as abscissa. The main factors affecting the yield envelope are temperature and strain rate, whereas particle cavitation is a function of particle size and the shear modulus of the rubber. Cavitation diagrams help in understanding the changes in materials behaviour observed as these factors are varied.

Over the past 20 years, numerous studies of rubber-toughened polymers have provided evidence of cavitation in the rubber particles, especially at or near fracture surfaces. The best-documented examples are in toughened epoxies[17,20–25], nylons[16,26–28] and polystyrene[29–32], but the list also includes acrylonitrile–butadiene–styrene (ABS) and poly(vinyl chloride) (PVC)[33]. Scanning and transmission electron microscopy, together with optical microscopy, have all proved useful in revealing patterns of cavitation. Most papers on the subject have made the point that rubber particle cavitation reduces the constraints on yielding imposed upon material at the tip of a sharp crack, especially in thick sections.

In addition to demonstrating particle cavitation, a number of published papers on rubber-toughened plastics include micrographs of dilatation bands[22–24,28]. In some cases, void formation shows no obvious pattern, while in others it is concentrated into well defined bands. Polarized light microscopy studies by Yee and Pearson[22,23] on toughened epoxy resin show that the yield zone contains a high density of shear bands, which run from one cavitated particle to another; and recent work by Sue[24] has demonstrated the formation in toughened epoxy resins of 'croids'—craze-like planar regions of cavitated particles lying ahead of an advancing crack.

There is an obvious relationship between Sue's 'croids' and the crazes reported by Argon *et al.*[31] in styrene–butadiene block copolymers, in which cavitation occurred quantitatively in small spheres or rods of polybutadiene, on planes normal to the applied tensile stress. Crazes of this type, which propagate by 'repeated cavitation of heterophases'[31], are different from conventional crazes, which contain interconnected voids formed through the meniscus instability mechanism.

Polymers appear to form a continuous spectrum of deformation bands, ranging from 'ordinary' crazes through dilatation bands of various sorts, to void-free shear bands. Each type of band is characterized by its angle to the applied stress, its void content and the degree of interconnection between voids. In this context, 'croids' and the crazes observed in styrene–butadiene–styrene (SBS) block copolymers can be recognized as particular types of dilatation band, which are similar in that they are formed on planes lying approximately normal to the applied tensile stress, and that there is little particle cavitation outside the well defined bands.

These observations can be understood in the light of equation (2). The materials used by both Sue and Argon *et al.* have very narrow distributions of particle size. Consequently, when one or two particles begin to cavitate, there are always other particles of similar size nearby, which are already close to the critical cavitational strain, and need only a small increase in local volume strain to initiate void formation. Thus the band will propagate along the preferred angle ψ. Because all of the particles within a given small zone tend to cavitate simultaneously under these conditions, the effective volume fraction of voids is high, and ψ is therefore close to zero. Where there is a wide distribution of particle sizes, much more scattered cavitation is to be expected, involving the largest rubber particles, and it may be more difficult to discern a spatial pattern.

The cavitation–dilatation band model provides a quantitative approach to yielding in toughened plastics, for those cases in which cavitation of the rubber particles is a contributory process. It relates the critical strain required for cavitation to the properties of the particle (size, shear modulus and failure strain in biaxial extension) without introducing arbitrary quantities. Many of the concepts embodied in the model have been discussed qualitatively by previous authors. In particular, many have recognized that particle cavitation has the beneficial effect of relieving the constraints at a crack tip. There have also been extensive studies by Gent and coworkers[8–12] relating to the critical mean stress required to cause cavitation in bulk samples of rubber. However, their analysis is based on the assumption that the rubber contains defects of specified dimensions, and is therefore difficult to apply to toughened plastics containing non-cavitated rubber particles. Attempts have been made to use Gent's criterion for defect growth in bulk rubbers ($\sigma_m = 5E/6$ at cavitation, where E is Young's modulus) to rubber particles in toughened plastics[27], but it does not account for important effects in rubber toughening, notably particle size effects. The new model overcomes these difficulties.

ACKNOWLEDGEMENTS

The authors thank the Science and Engineering Research Council (GR/H06354) and MURST (60%) for financial support of this project. They also thank Drs R. J.

Gaymans and K. Dijkstra for providing toughened nylon samples.

REFERENCES

1 Lazzeri, A. and Bucknall, C. B. *J. Mater. Sci.* 1993, **28,** 6799
2 McClintock, F. A. *J. Appl. Mech.* 1968, **90,** 362
3 Berg, C. A. 'Inelastic Behaviour of Solids' (Eds. J. R. Rice and M. A. Johnson), McGraw-Hill, New York, 1970
4 Gurson, A. L. ICF4 Fracture 1977, Waterloo, Canada (Ed. D. M. R. Taplin), Vol. 2A, Pergamon, Oxford, 1977, p. 357
5 Tvergaard, V. *Int. J. Fract.* 1988, **55,** 126
6 Dung, N. L. *Int. J. Fract.* 1992, **53,** R19
7 Thomason, P. F. 'Ductile Fracture of Metals', Pergamon, Oxford, 1991
8 Gent, A. N. and Lindley, P. B. *Proc. R. Soc. (A)* 1959, **249,** 195
9 Gent, A. N. and Tompkins, D. A. *J. Appl. Phys.* 1959, **40,** 2520
10 Gent, A. N. and Park, B. *J. Mater. Sci.* 1984, **19,** 1947
11 Cho, K. and Gent, A. N. *J. Mater. Sci.* 1988, **23,** 141
12 Gent, A. N. and Wang, C. *J. Mater. Sci.* 1991, **26,** 3392
13 Williams, M. L. and Schapery, R. A. *Int. J. Fract. Mech.* 1965, **1,** 64
14 Bucknall, C. B., Karpodinis, A. M. and Zhang, X. C. *J. Mater. Sci.* 1994, **29,** 3377
15 Ward, I. M. 'Mechanical Properties of Solid Polymers', 2nd Edn., Wiley, New York, 1983, pp. 361–2
16 Dijkstra, K. PhD Thesis, University of Twente, Netherlands, 1993
17 Huang, Y. and Kinloch, A. J. *J. Mater. Sci. Lett.* 1992, **11,** 1947
18 Gloaguen, J. M., Heim, P., Gaillard, P. and Lefebvre, J. M. *Polymer* 1992, **33,** 4741
19 Bucknall, C. B. 'Toughened Plastics', Applied Science, London, 1977
20 Bascom, W. D., Cottington, R. L. and Siebert, A. *Appl. Polym. Symp.* 1977, **32,** 165
21 Kinloch, A. J., Shaw, S. J., Tod, D. A. and Hunston, D. L. *Polymer* 1983, **24,** 1341
22 Pearson, R. A. and Yee, A. F. *J. Mater. Sci.* 1986, **21,** 2475
23 Yee, A. F. and Pearson, R. A. 'Fractography and Failure Mechanisms in Polymers and Composites' (Ed. A. C. Roulin-Moloney), Elsevier, London, 1989
24 Sue, H. Y. *J. Mater. Sci.* 1992, **27,** 3098
25 Huang, Y. and Kinloch, A. J. *J. Mater. Sci. Lett.* 1984, **11,** 1947
26 Ramsteiner, F. and Heckmann, W. *Polym. Commun.* 1985, **26,** 199
27 Bucknall, C. B., Heather, P. S. and Lazzeri, A. *J. Mater. Sci.* 1989, **24,** 1489
28 Speroni, F., Castoldi, E., Fabbri, P. and Casiraghi, T. *J. Mater. Sci.* 1989, **24,** 2165
29 Beahan, P., Thomas, A. and Bevis, M. *J. Mater. Sci.* 1976, **11,** 1207
30 Donald, A. M. and Kramer, E. J. *J. Appl. Polym. Sci.* 1982, **27,** 3729
31 Argon, A. S., Cohen, R. E., Gebizlioglu, O. S. and Schwier, C. E. 'Advances in Polymer Science,' Vols. 52/53, (Ed. H. H. Kausch), Springer, Heidelberg, 1983
32 Michler, G. H. *Acta Polym.* 1985, **36,** 285
33 Breuer, H., Haaf, F. and Stabenow, J. *J. Macromol. Sci.–Phys. (B)* 1977, **14,** 387